

# A. Appendix

In the Appendix we will derive in detail the numerical discretization scheme for the committor equation associated with the Smoluchowski and Langevin dynamics, respectively. The main challenge will be to devise a stable finite difference scheme for the hypoelliptic committor equation. In Section A.3, we will prove the existence and uniqueness of a weak solution of the elliptic mixed-boundary value problem associated with the elliptic committor equation. Moreover, we will explain the link between the derived discretization schemes and the approximation of diffusion processes via Markov jump processes. We will end the Appendix by giving definitions and the technical proofs for the probability current of reactive trajectories and the expression for their rate.

## A.1. Discretization of the Committor Equation

For the sake of a compact notation, we will write the (forward) committor equation (3.6) in the following form

$$\begin{cases} \mathcal{L}_{bw}q = 0 & \text{in } \mathbb{R}^d \setminus \mathcal{S} \\ q = g_D & \text{on } \partial\mathcal{S} \end{cases}$$

where  $\mathcal{L}_{bw}$  is the generator of the considered Markov diffusion process, the set  $\mathcal{S} = A \cup B$  is the union of two disjoint closed sets  $A, B \subset \mathbb{R}^d$  and the Dirichlet condition on the boundary  $\partial\mathcal{S}$  is given by the function  $g_D : \partial\mathcal{S} \rightarrow \mathbb{R}$ , defined according to

$$g_D(x) = \begin{cases} 0, & \text{if } x \in \partial A \\ 1, & \text{if } x \in \partial B. \end{cases} \quad (\text{A.1})$$

The numerical treatment of the committor equation requires the choice of a bounded discretization domain  $\Omega \subset \mathbb{R}^d$  such that the probability to find the equilibrated diffusion process in  $\Omega$  is almost one. As explained in Section 2.1.9, the restriction of the diffusion process on  $\Omega$  leads to additional conditions for the committor function  $q(x)$  on the boundary  $\partial\Omega$ , that are

$$0 = a\nabla q \cdot \hat{n} = \nabla q \cdot a\hat{n}, \quad (\text{A.2})$$

where  $a(x)$  is the diffusion matrix and  $\hat{n}$  is the unit normal on  $\partial\Omega$  pointing outward  $\Omega$ . Hence, the committor function  $q(x)$  considered on a domain  $\Omega$  has to satisfy the *mixed-boundary value problem*

$$\begin{cases} \mathcal{L}_{bw}q = 0 & \text{in } \Omega_{\mathcal{S}} \\ q = g_D & \text{on } \partial\mathcal{S} \\ \nabla q \cdot a\hat{n} = 0 & \text{on } \partial\Omega. \end{cases} \quad (\text{A.3})$$

## A. Appendix

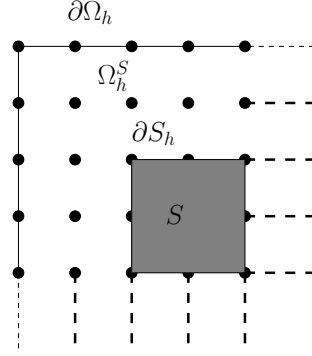


Figure A.1.: Schematic representation of the mesh  $\overline{\Omega_h^S}$  and its disjoint boundaries  $\partial \Omega_h$  and  $\partial S_h$ .

### A.1.1. Discretization via Finite Differences

In this section we will introduce the framework for the finite difference discretization of the mixed-boundary value problem (A.3) on a two dimensional domain  $\Omega \subset \mathbb{R}^2$ .

**Remark A.1.1.** *We will consider only rectangular domains with boundaries which are piecewise parallel to the axis of the coordinate system. Furthermore, we assume that the shape of the sets  $A$  and  $B$  are such that their boundaries  $\partial A$  and  $\partial B$  can be discretized by an appropriate discretization of the domain. The reasons for that restrictions are:*

- *The results of TPT for diffusion processes on rectangular domains already demonstrate the ability of TPT to capture different dynamical scenarios.*
- *The schemes are straightforward to derive and are easy to implement.*
- *The treatment of general domains and sets  $A$  and  $B$  would go beyond the scope of this thesis.*

#### Discretization of the Domain

Let  $\Omega = (a, b) \times (c, d) \subset \mathbb{R}^2$ ,  $a < b, c < d$ . be a rectangular domain. We discretize  $\Omega$  by a uniform mesh which is defined by

$$\begin{aligned} \Omega_h &\stackrel{def}{=} \{\mathbf{x} = (a + ih_x, b + jh_y) : 1 < i < N - 1, 1 < j < M - 1\}, \\ \partial \Omega_h &\stackrel{def}{=} \{\mathbf{x} = (a + ih_x, b + jh_y) : 0 \leq i \leq N, 0 \leq j \leq M\} \setminus \Omega_h, \end{aligned}$$

where  $h = (h_x, h_y)$  and, e.g.,  $h_x = (b - a)/(N + 1)$  is the mesh width in  $x$ -direction and  $N + 1$  is the number of mesh points in  $x$ -direction. Next, we assume that the boundary  $\partial S$  of the set  $S$  can be represented as a closed polygon which is piecewise parallel with respect to the axes of the coordinate system. We discretize the set  $S$  by

$$\mathcal{S}_h \stackrel{def}{=} \Omega_h \cap S$$

and denote its complement with respect to the mesh  $\Omega_h$  by

$$\Omega_h^S \stackrel{def}{=} \Omega_h \setminus \mathcal{S}_h.$$

### A.1. Discretization of the Committor Equation

Moreover, the boundary  $\partial\mathcal{S}_h$  of  $\mathcal{S}_h$  is defined by (cf. A.1.1)

$$\partial\mathcal{S}_h \stackrel{def}{=} \Omega_h \cap \partial\mathcal{S}.$$

The boundary conditions on the disjoint boundaries  $\partial\Omega$  and  $\partial\mathcal{S}$  requires the incorporation of their respective discretizations  $\partial\Omega_h$  and  $\partial\mathcal{S}_h$  into the mesh  $\Omega_h^{\mathcal{S}}$ . We define

$$\begin{aligned} \overline{\Omega}_h^{\mathcal{S}} &\stackrel{def}{=} \Omega_h^{\mathcal{S}} \cup \partial\Omega_h, \\ \overline{\Omega}_h^{\mathcal{S}} &\stackrel{def}{=} \Omega_h^{\mathcal{S}} \cup \partial\Omega_h \cup \partial\mathcal{S}_h. \end{aligned}$$

In Figure A.1 we give a schematic representation of the mesh  $\overline{\Omega}_h^{\mathcal{S}}$  and its disjoint boundaries  $\partial\Omega_h$  and  $\partial\mathcal{S}_h$ .

#### Restrictions

For the proof of consistency and stability it is convenient to introduce an operator which restricts a continuous function onto the mesh  $\Omega_h^{\mathcal{S}}$ . Let  $u : \mathbb{R}^2 \rightarrow \mathbb{R}$  then we define the restriction  $R_h^{\mathcal{S}} : u \mapsto \mathbb{R}^{|\Omega_h^{\mathcal{S}}|}$  by

$$(R_h^{\mathcal{S}}u)(\mathbf{x}) \stackrel{def}{=} u(\mathbf{x}) \quad \forall \mathbf{x} \in \Omega_h^{\mathcal{S}}.$$

The restriction  $\overline{R}_h^{\mathcal{S}}$  with respect to the mesh  $\overline{\Omega}_h^{\mathcal{S}}$  and  $\overline{R}_h^{\mathcal{S}}$  with respect to the mesh  $\overline{\Omega}_h^{\mathcal{S}}$  is defined analogously. We call a function  $u_h$  a *mesh function* if  $u_h$  is only defined on a mesh.

#### Discretization Matrix and Elimination of Boundary Conditions

In the following,  $D_h \in \mathbb{R}^{|\Omega_h^{\mathcal{S}}| \times |\overline{\Omega}_h^{\mathcal{S}}|}$  denotes the matrix which results from the discretization of the operator  $\mathcal{L}_{bw}$  on the mesh  $\Omega_h^{\mathcal{S}}$  under consideration of the mesh points in  $\overline{\Omega}_h^{\mathcal{S}}$  where, e.g.  $|\Omega_h^{\mathcal{S}}|$  is the number of mesh points in  $\Omega_h^{\mathcal{S}}$ . One option to deal with the Neumann boundary conditions on  $\partial\Omega$  is their incorporation into the discretization stencils of the operator  $\mathcal{L}_{bw}$  for mesh points in the direct vicinity of the boundary  $\partial\Omega_h$ . Since we deal here with homogeneous Neumann boundary conditions, we chose an alternative option. Here we discretize the Neumann conditions on  $\partial\Omega_h$  explicitly and denote the resulting matrix by  $N_h \in \mathbb{R}^{|\partial\Omega_h| \times |\overline{\Omega}_h^{\mathcal{S}}|}$ . Combining both matrices in one matrix, we end up with

$$\overline{D}_h \stackrel{def}{=} \begin{pmatrix} D_h \\ N_h \end{pmatrix} \in \mathbb{R}^{|\overline{\Omega}_h^{\mathcal{S}}| \times |\overline{\Omega}_h^{\mathcal{S}}|}. \quad (\text{A.4})$$

Let  $u_h$  be a mesh function on  $\overline{\Omega}_h^{\mathcal{S}}$ . If we apply the vector  $u_h$  on the matrix  $D_h$ , then the entry  $(D_h u_h)(\mathbf{x})$  corresponding to a mesh point  $\mathbf{x} \in \Omega_h^{\mathcal{S}}$  can be written as

$$(D_h u_h)(\mathbf{x}) = \sum_{\mathbf{y} \in \Omega_h^{\mathcal{S}}} D_h(\mathbf{x}, \mathbf{y}) u_h(\mathbf{y}) + \sum_{\mathbf{z} \in \partial\mathcal{S}_h} D_h(\mathbf{x}, \mathbf{z}) u(\mathbf{z}). \quad (\text{A.5})$$

## A. Appendix

If we assume that  $u_h(\mathbf{z}) = g_D(\mathbf{z})$  for all  $\mathbf{z} \in \partial\Omega_h$ , then (A.5) reduces to

$$(D_h u_h)(\mathbf{x}) = (L_h u_h)(\mathbf{x}) + \sum_{\mathbf{z} \in \partial\mathcal{S}_h} D_h(\mathbf{x}, \mathbf{z}) g_D(\mathbf{z}),$$

where  $(L_h u_h)(x)$  is a compact notation for the first sum in (A.5). Finally, we can write the finite difference discretization of the mixed-boundary value problem (A.3) *after* elimination of the Dirichlet boundary conditions as the following linear system

$$\bar{L}_h u_h = \bar{F}_h,$$

where the matrix on the left hand side is defined by

$$\bar{L}_h \stackrel{def}{=} \begin{pmatrix} L_h \\ N_h \end{pmatrix} \in \mathbb{R}^{|\bar{\Omega}_h^S| \times |\bar{\Omega}_h^S|} \quad (\text{A.6})$$

and for  $\mathbf{x} \in \bar{\Omega}_h^S$  the right hand side is given by

$$\bar{F}_h(\mathbf{x}) = \begin{cases} -\sum_{\mathbf{z} \in \partial\mathcal{S}_h} D_h(\mathbf{x}, \mathbf{z}) g_D(\mathbf{z}), & \text{if } \mathbf{x} \in \Omega_h^S \\ 0, & \text{if } \mathbf{x} \in \partial\Omega_h. \end{cases}$$

### A.1.2. Finite Difference Discretization of the Smoluchowski Committor Equation

In this section, we state a stable finite difference scheme of the committor equation for the Smoluchowski dynamics (2.37) on a two dimensional domain  $\Omega \subset \mathbb{R}^2$ . The associated mixed-boundary value problem (A.3) reduces to the problem

$$\begin{cases} \mathcal{L}_{bw} q = 0 & \text{in } \Omega_S \\ q = g_D & \text{on } \partial\mathcal{S} \\ \frac{\partial q}{\partial \hat{n}} = 0 & \text{on } \partial\Omega, \end{cases} \quad (\text{A.7})$$

where the operator  $\mathcal{L}_{bw}$ , given by

$$\mathcal{L}_{bw} q = \beta^{-1} \Delta q - \nabla V \cdot \nabla q$$

is an *elliptic* linear second order partial differential operator. Notice, that for the sake of simplicity, we set the friction matrix  $\Gamma = \text{diag}(1, 1) \in \mathbb{R}^{2 \times 2}$ .

There is a long list of literature on stable finite difference discretization schemes of elliptic partial differential operators, e.g. [44, 42]. The discretization schemes we use here are standard schemes which are found in, e.g. [44].

### Finite Difference Scheme

For notational simplicity, we henceforth assume that the mesh  $\Omega_h$  is *total uniform*, i.e.  $h_x = h_y$ . Let  $\mathbf{x} \in \Omega_h^S$  then we discretize the elliptic operator  $\mathcal{L}_{bw}$  in  $\mathbf{x}$  by the 5-point stencil

$$\beta^{-1} h^{-2} \begin{bmatrix} 0 & 1 & 0 \\ 1 & -4 & 1 \\ 0 & 1 & 0 \end{bmatrix} + (2h)^{-1} \begin{bmatrix} 0 & v_2 & 0 \\ -v_1 & 0 & v_1 \\ 0 & -v_2 & 0 \end{bmatrix}, \quad (\text{A.8})$$

### A.1. Discretization of the Committor Equation

where we set  $(v_1, v_2) = -\nabla V(\mathbf{x})$  and  $h = h_x = h_y$ . The stencil (A.8) leads to a consistent scheme of second order, i.e. for a function  $u \in C^2(\Omega)$  we have

$$\left\| D_h \overline{R}_h^S u - R_h^S \mathcal{L}_{bw} u \right\|_\infty = \mathcal{O}(h^2). \quad (\text{A.9})$$

For reasons of stability, we have to ensure that all off-diagonal entries in the resulting discretization matrix  $L_h$  are non-negative. This leads to a condition on the mesh width  $h$ , namely

$$h < 2\beta^{-1} \left( \max_{\mathbf{x} \in \Omega_h^S} \{|v_1|, |v_2| : (v_1, v_2) = -\nabla V(\mathbf{x})\} \right)^{-1}. \quad (\text{A.10})$$

We discretize the Neumann conditions on  $\partial\Omega$  explicitly by a single sided difference scheme. For example, consider a mesh point  $\mathbf{x} = (x, y) \in \partial\Omega_h$  on the left boundary, i.e. the piece of the boundary  $\partial\Omega$  which confines the rectangular domain  $\Omega$  from the left and let  $\hat{n}(x, y) \equiv (-1, 0)$  be the corresponding unit normal vector pointing outward  $\Omega$ . To ensure the M-matrix property and without lack of generality, we discretize the Neumann conditions in the boundary mesh point  $\mathbf{x} = (x, y)$  by

$$\frac{\partial}{\partial \hat{n}(x, y)} q(x, y) = 0 \rightsquigarrow h^{-1}(q(x-h, y) - q(x, y)) = 0$$

which is represented by the stencil

$$h^{-1} \begin{bmatrix} 0 & 0 & 0 \\ 1 & -1 & 0 \\ 0 & 0 & 0 \end{bmatrix}. \quad (\text{A.11})$$

The stencils for the right, upper and lower boundaries are derived analogously. Notice that the stencils in the corners result from the combination of the stencils of the two adjacent boundaries. For example, for the upper-right corner the stencil takes the form

$$h^{-1} \begin{bmatrix} 0 & 0 & 0 \\ 1 & -2 & 0 \\ 0 & 1 & 0 \end{bmatrix}. \quad (\text{A.12})$$

#### Properties of the Discretization Matrix

As a preparation for the proof of stability, we show that the discretization matrix  $\overline{L}_h$  (after elimination of the Dirichlet boundary conditions) is up to its sign an M-matrix. To be more precise, the following properties hold for the matrix  $-\overline{L}_h$ :

1. For a mesh point  $\mathbf{x} \in \Omega_h^S$  in the direct vicinity of the boundary  $\partial\mathcal{S}_h$  the following strict inequality holds

$$|\overline{L}_h(\mathbf{x}, \mathbf{x})| > \sum_{\substack{\mathbf{y} \in \Omega_h^S \\ \mathbf{y} \neq \mathbf{x}}} |\overline{L}_h(\mathbf{x}, \mathbf{y})|.$$

## A. Appendix

2. The entries of the matrix  $-\bar{L}_h$  satisfy the following sign conditions

$$\begin{aligned} -\bar{L}_h(\mathbf{x}, \mathbf{x}) &> 0, \quad \forall \mathbf{x} \in \Omega_h^S, \\ -\bar{L}_h(\mathbf{x}, \mathbf{y}) &\leq 0, \quad \forall \mathbf{x}, \mathbf{y} \in \Omega_h^S, \mathbf{x} \neq \mathbf{y}. \end{aligned} \quad (\text{A.13})$$

which immediately follow from the discretization schemes (A.8) and (A.11).

3. Under the assumption that  $\Omega \setminus (A \cup B)$  is connected, the matrix  $-\bar{L}_h$  is essentially diagonally dominant.

Finally, from Theorem (A.6.6) it follows that the matrix  $-\bar{L}_h$  is an M-matrix and in particular invertible.

### Proof of Stability

To prove that our scheme is stable, we have to show

$$\sup_{h>0} \left\| \bar{L}_h^{-1} \right\|_{\infty} < \infty.$$

To be more precise, we have to show that there exists a constant  $C > 0$  and a sufficiently small  $h_0 > 0$  such that

$$\left\| L_h^{-1} \right\|_{\infty} \leq C, \quad \forall h \in (0, h_0). \quad (\text{A.14})$$

The idea of the proof is to find a function  $s \in C^2(\Omega) \cap C^1(\bar{\Omega})$  and a sufficiently small  $h_0 > 0$  such that we have

$$(-\bar{L}_h \bar{R}_h^S s)(\mathbf{x}) \geq 1, \quad \forall \mathbf{x} \in \bar{\Omega}_h^S, \forall h \in (0, h_0). \quad (\text{A.15})$$

Then by virtue of Theorem A.6.7 we deduce the desired result (A.14).

In the case of a pure elliptic Dirichlet boundary value problem, one can state explicitly a function  $s(x)$  which leads to (A.15) (see [44], Theorem 5.1.9.). Unfortunately, in our case of the mixed-boundary value problem (A.7) we cannot state such a function explicitly. Instead, we consider the following auxiliary mixed-boundary value problem

$$\begin{cases} \mathcal{L}_{bw} s = -1 & \text{in } \Omega_S \\ s = 0 & \text{on } \partial S \\ \frac{\partial s}{\partial \hat{n}} = -1 & \text{on } \partial \Omega, \end{cases} \quad (\text{A.16})$$

where the operator  $\mathcal{L}_{bw}$  is again the generator of the Smoluchowski dynamics and we show that a solution  $s(x) \in C^2(\Omega) \cap C^1(\bar{\Omega})$  of (A.16) is the right candidate to deduce (A.15). For an interpretation of the solution of (A.16) see Remark A.1.2.

**Theorem A.1.1.** *The discretization scheme (A.8) and (A.11) is stable. The stability constant is given by*

$$C = 2 \max_{x \in \bar{\Omega} \setminus \mathcal{S}} \{|s(x)|\},$$

where the function  $s(x)$  is the solution of the problem (A.16).

### A.1. Discretization of the Committor Equation

*Proof.* Let  $s(x) \in C^2(\Omega) \cap C^1(\bar{\Omega})$  be the solution of the stability equation (A.16). We define the auxiliary mesh function  $u_h = 2\overline{R_h^S} s$  and we deduce

$$\begin{aligned} -D_h u_h &= -2(D_h \overline{R_h^S} s - R_h^S \mathcal{L}_{bw} s) - 2R_h^S \mathcal{L}_{bw} s \\ &= 2 - 2(D_h \overline{R_h^S} s - R_h^S \mathcal{L}_{bw} s) \end{aligned}$$

From the consistency of our scheme follows that there exists an  $h_0 > 0$  such that

$$\left\| D_h \overline{R_h^S} s - R_h^S \mathcal{L}_{bw} s \right\|_\infty < \frac{1}{2}, \quad \forall h \in (0, h_0)$$

and we deduce

$$(-D_h u_h)(\mathbf{x}) \geq 1, \quad \forall \mathbf{x} \in \Omega_h^S, \quad \forall h \in (0, h_0).$$

But this immediately implies

$$(-\bar{L}_h u_h)(\mathbf{x}) \geq 1, \quad \forall h \in (0, h_0)$$

for any mesh point  $\mathbf{x} \in \Omega_h^S$  which is not in the direct vicinity of the boundary  $\partial A_h \cup \partial B_h$ . Next, consider a mesh point  $\mathbf{x} \in \Omega_h^S$  which is in the direct vicinity of the boundary  $\partial A_h \cup \partial B_h$ . But since the function  $s(\mathbf{x})$  is equal to zero on the boundary of the set  $\mathcal{S}$  we have

$$\sum_{\mathbf{y} \in (\partial S)_h} D_h(\mathbf{x}, \mathbf{y}) u_h(\mathbf{y}) = 0$$

and, thus, we finally obtain

$$(-\bar{L}_h u_h)(\mathbf{x}) = (-L_h u_h)(\mathbf{x}) \geq 1 \quad \forall \mathbf{x} \in \Omega_h^S, \forall h \in (0, h_0). \quad (\text{A.17})$$

It remains to show that (A.17) also holds true for mesh points on the boundary  $\partial \Omega_h$ . But since the matrix  $N_h$  results from the consistent discretization of the Neumann condition, the same reasoning as above yields that there exists an  $\tilde{h}_0 > 0$  such that

$$(-\bar{L}_h u_h)(\mathbf{x}) = -(N_h u_h)(\mathbf{x}) \geq 1 \quad \forall \mathbf{x} \in \partial \Omega_h, \forall h \in (0, \tilde{h}_0).$$

All together we have shown that

$$(-\bar{L}_h u_h)(\mathbf{x}) \geq 1 \quad \forall \mathbf{x} \in \bar{\Omega}_h^S, 0 < h < \min\{h_0, \tilde{h}_0\}$$

and by Theorem (A.6.7) we obtain

$$\left\| \bar{L}_h^{-1} \right\|_\infty \leq \|u_h\|_\infty \leq 2 \max_{x \in \bar{\Omega} \setminus \mathcal{S}} \{|s(x)|\} < \infty, \quad 0 < h < \min\{h_0, \tilde{h}_0\}.$$

□

**Remark A.1.2.** *The stability equation (A.16) admits a partial interpretation if one realizes that its solution  $s(x)$  can be decomposed such that*

$$s(x) = s_1(x) + s_2(x),$$

## A. Appendix

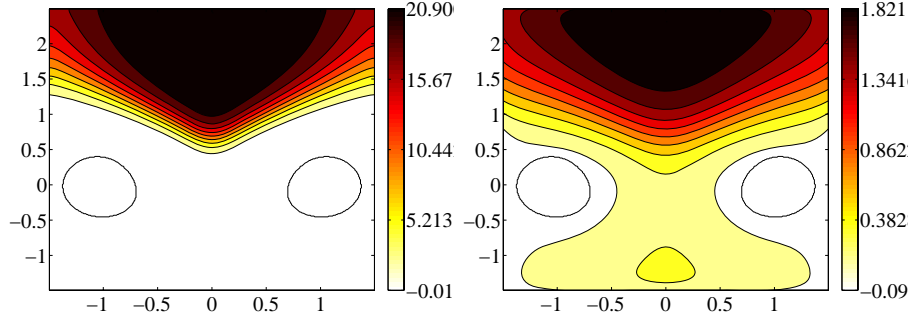


Figure A.2.: Contour plot of the numerical solution  $|s(x)|$  of the mixed-boundary value problem (A.16) for the Smoluchowski dynamics in the three-hole potential (given in (3.45)) for a low temperature  $\beta = 6.67$  (left panel) and for a high temperature  $\beta = 1.67$  (right panel).

where the function  $s_1$  is the solution of the problem

$$\begin{cases} \mathcal{L}_{bw}s_1 = -1 & \text{in } \Omega_S \\ s_1 = 0 & \text{on } \partial\mathcal{S} \\ \frac{\partial s_1}{\partial \hat{n}} = 0 & \text{on } \partial\Omega \end{cases} \quad (\text{A.18})$$

and the function  $s_2(x)$  satisfies

$$\begin{cases} \mathcal{L}_{bw}s_2 = 0 & \text{in } \Omega_S \\ s_2 = 0 & \text{on } \partial\mathcal{S} \\ \frac{\partial s_2}{\partial \hat{n}} = -1 & \text{on } \partial\Omega. \end{cases} \quad (\text{A.19})$$

As shown in Remark (3.1.2), the function  $s_1(x)$  is the **mean first passage time** of the Smoluchowski dynamics (2.37) with respect to the set  $A \cup B$ . In Figure A.2 we show the contour plot of the numerical solution  $s(x)$  of the equation in (A.16) for the Smoluchowski dynamics in the three-hole potential (3.45) (see section (3.7.1)) for two different temperatures.

### Proof of Convergence

For the convenience of the reader, we state the proof that our scheme converges which, as usual, follows from the consistency and stability.

**Theorem A.1.2.** *Let  $u$  be the exact solution of the mixed-boundary value problem (A.7) and let  $\bar{u}_h$  denote the approximated solution computed via  $\bar{u}_h = \bar{L}_h^{-1} \bar{F}_h$ . Then we have*

$$\lim_{h \rightarrow 0} \left\| \bar{u}_h - \bar{R}_h^S u \right\|_{\infty} = 0$$

*Proof.* Let  $\tilde{u}_h$  be the extension of the mesh function  $\bar{u}_h$  on the boundary of  $\mathcal{S}$ , that is

$$\tilde{u}_h(\mathbf{x}) \stackrel{\text{def}}{=} \begin{cases} \bar{u}_h(\mathbf{x}), & \text{if } \mathbf{x} \in \bar{\Omega}_h^S \\ g_D(\mathbf{x}), & \text{if } \mathbf{x} \in \partial\mathcal{S}_h \end{cases}$$



### A.1. Discretization of the Committor Equation

Next, we define the auxiliary mesh function  $w_h = \tilde{u}_h - \overline{R}_h^{\mathcal{S}}u$  and deduce

$$\overline{D}_h w_h = \overline{L}_h(\tilde{u}_h - \overline{R}_h^{\mathcal{S}}u)$$

because of  $w_h(\mathbf{x}) = 0$  on the boundary of  $\mathcal{S}$ . Now we can estimate the cut-off error by

$$\begin{aligned} \left\| \tilde{u}_h - \overline{R}_h^{\mathcal{S}}u \right\|_{\infty} &= \left\| \overline{L}_h^{-1} \overline{D}_h w_h \right\|_{\infty} \\ &\leq \left\| \overline{L}_h^{-1} \right\|_{\infty} \cdot \left\| \overline{D}_h(\tilde{u}_h - \overline{R}_h^{\mathcal{S}}u) \right\|_{\infty} \\ &\leq C \cdot \max \left\{ \left\| D_h \tilde{u}_h - D_h \overline{R}_h^{\mathcal{S}}u \right\|_{\infty}, \left\| N_h \tilde{u}_h - N_h \overline{R}_h^{\mathcal{S}}u \right\|_{\infty} \right\}, \end{aligned}$$

where the last inequality follows from the stability of the scheme and the definition of the matrix  $\overline{D}_h$  (cf. (A.4)). Now observe that

$$\begin{aligned} (D_h \tilde{u}_h)(\mathbf{x}) &= (R_h^{\mathcal{S}} \mathcal{L}_{bw} u)(\mathbf{x}) \quad \forall \mathbf{x} \in \Omega_h^{\mathcal{S}}, \\ (N_h \tilde{u}_h)(\mathbf{x}) &= (\overline{R}_h^{\mathcal{S}} \frac{\partial u}{\partial \hat{n}})(\mathbf{x}) \quad \forall \mathbf{x} \in \partial \Omega_h, \end{aligned}$$

and, hence, since the schemes are consistent, we finally get

$$\left\| \tilde{u}_h - \overline{R}_h^{\mathcal{S}}u \right\|_{\infty} \longrightarrow 0 \text{ as } h \rightarrow 0$$

which completes the proof.  $\square$

#### A.1.3. Finite Difference Discretization of the Langevin Committor Equation

In this section we derive a stable finite difference scheme of the forward committor equation for the Langevin dynamics (2.33) on a two dimensional domain  $\Omega \subset \mathbb{R}^2$ . For the sake of simplicity, we set the mass equal to one ( $m_1 = 1$ ) and consider the velocity instead of the momentum. The mixed-boundary value problem (A.3) reduces to the problem

$$\begin{cases} \mathcal{L}_{bw} q = 0 & \text{in } \Omega^{\mathcal{S}} = \Omega \setminus \mathcal{S} \\ q = g_D & \text{on } \partial \mathcal{S} \\ \nabla q \cdot a \hat{n} = 0 & \text{on } \partial \Omega, \end{cases} \quad (\text{A.20})$$

where the operator  $\mathcal{L}_{bw}$ , given by

$$\mathcal{L}_{bw} q = \gamma \beta^{-1} \Delta_v q + v \cdot \nabla_x q - \nabla_x V \cdot \nabla_v q - \gamma v \cdot \nabla_v q, \quad (\text{A.21})$$

is a degenerate elliptic linear second order partial differential operator.

In contrast to the Smoluchowski dynamics where the involved operator is elliptic, here the degenerate ellipticity of  $\mathcal{L}_{bw}$  imposes geometric restrictions of the domain  $\Omega$ . Recalling that the diffusion matrix for the Langevin dynamics on a two-dimensional phase space is given by

$$a = \beta^{-1} \gamma \begin{pmatrix} 0 & 0 \\ 0 & 1 \end{pmatrix} \in \mathbb{R}^{2 \times 2},$$

## A. Appendix

the Neumann conditions for the forward committor function  $q(x, v)$  in a boundary point  $(x, v) \in \partial\Omega$  reduces to

$$0 = \nabla q(x, v) \cdot a\hat{n} = \frac{dq(x, v)}{dv} \hat{n}_v,$$

where  $\hat{n} = (\hat{n}_x, \hat{n}_v)^T$  is the unit normal in  $(x, v) \in \partial\Omega$  pointing outward  $\Omega$ . But this immediately implies that if the shape of boundary in the  $(x, v)$  was such that  $\hat{n}_v = 0$  then this would lead to an empty boundary condition in that point and the resulting linear system would be under-determined. Consequently, any domain  $\Omega$  whose boundary consists of pieces which are parallel to the  $v$ -axis is inappropriate for the finite difference discretization. Furthermore, in order to be able to impose the Dirichlet boundary conditions on  $\partial A$  and  $\partial B$ , the unit normal to these sets at  $(x, v)$  must span the velocity degrees of freedom everywhere except maybe on a set of zero measure on  $\partial A$  and  $\partial B$ . One option could be to change the shape the domain and the sets  $A$  and  $B$  such that their boundaries are not piecewise parallel to the  $v$ -axis. But this option would lead to complicated finite difference schemes for the boundary conditions and, hence, it seems not practical.

As a remedy, we introduce a coordinate transformation such that

1. the transformed Langevin dynamics exhibits diffusion in *all* new coordinates,
2. the Neumann boundary conditions for a rectangular domain in the new coordinate system lead to non-empty conditions on the committor function.

To this end, we rotate the coordinate system by  $\pi/4$  which can formally be done by introducing the transformation  $T : (x, v) \mapsto (\eta(x, v), \xi(x, v))$  with

$$\begin{cases} \eta(x, v) = c(x - v), \\ \xi(x, v) = c(x + v), \quad c = \sqrt{2}/2. \end{cases} \quad (\text{A.22})$$

Then the Langevin dynamics in the new coordinates  $(\eta, \xi)$  takes the form

$$\begin{cases} d\eta = c^2(\xi - \eta)(1 + \gamma) + c\nabla_x V(c(\eta + \xi)) - c\sqrt{2\gamma\beta^{-1}} dW_t \\ d\xi = c^2(\xi - \eta)(1 - \gamma) - c\nabla_x V(c(\eta + \xi)) + c\sqrt{2\gamma\beta^{-1}} dW_t \end{cases} \quad (\text{A.23})$$

where  $W_t$  is a 1-dimensional Wiener process and affects both coordinates simultaneously. Now notice that the transformed dynamics (A.23) can be written in the shape of (2.8) by setting

$$\mathbf{b}(\eta, \xi) = \begin{pmatrix} c^2(\xi - \eta)(1 + \gamma) + c\nabla_x V(c(\eta + \xi)) \\ c^2(\xi - \eta)(1 - \gamma) - c\nabla_x V(c(\eta + \xi)) \end{pmatrix}, \quad c = \sqrt{2}/2 \quad (\text{A.24})$$

and

$$\sigma = c\sqrt{2\gamma\beta^{-1}} \begin{pmatrix} 0 & -1 \\ 0 & 1 \end{pmatrix}.$$

The generator  $\mathfrak{L}_{bw}$  of the transformed Langevin dynamics (A.23) is given by

$$\mathfrak{L}_{bw}u(\eta, \xi) = \mathbf{a} : \nabla\nabla u(\eta, \xi) + \mathbf{b}(\eta, \xi) \cdot \nabla u(\eta, \xi) \quad (\text{A.25})$$

### A.1. Discretization of the Committor Equation

with the diffusion matrix

$$\mathbf{a} = c^2 \gamma \beta^{-1} \begin{pmatrix} 1 & -1 \\ -1 & 1 \end{pmatrix}.$$

Notice that here  $\nabla = (\nabla_\eta, \nabla_\xi)$ . Finally, we end up with the mixed-boundary value problem in the new coordinates, that is

$$\begin{cases} \mathfrak{L}_{bw} q = 0 & \text{in } T(\Omega) \setminus T(\mathcal{S}) \\ q = \tilde{g}_D & \text{on } \partial T(\mathcal{S}) \\ \nabla q \cdot \mathbf{a} \hat{n} = 0 & \text{on } \partial T(\Omega) \end{cases} \quad (\text{A.26})$$

where  $\tilde{g}_D(x) = g_D(T^{-1}(x))$ .

The same reasoning as above leads to the mixed-boundary value problem associated with the backward committor equation

$$\begin{cases} \mathfrak{L}_{bw}^R q_b = \mathbf{a} : \nabla \nabla q_b + \mathbf{b}^R \cdot \nabla q_b = 0 & \text{in } T(\Omega) \setminus T(\mathcal{S}) \\ q_b = 1 - \tilde{g}_D & \text{on } \partial T(\mathcal{S}) \\ \nabla q_b \cdot \mathbf{a} \hat{n} = 0 & \text{on } \partial T(\Omega), \end{cases} \quad (\text{A.27})$$

where the reversed drift field  $\mathbf{b}^R(\eta, \xi)$  is given by

$$\mathbf{b}^R(\eta, \xi) = - \begin{pmatrix} c^2(\xi - \eta)(1 - \gamma) + c \nabla_x V(c(\eta + \xi)) \\ c^2(\xi - \eta)(1 + \gamma) - c \nabla_x V(c(\eta + \xi)) \end{pmatrix}, \quad c = \sqrt{2}/2. \quad (\text{A.28})$$

**Remark A.1.3.** *In order to keep the notation simple, we do not introduce a new symbol for the transformed domain  $T(\Omega)$  as well as for  $T(\mathcal{S})$ . In what follows,  $\Omega$  and  $\mathcal{S}$  are sets with respect to the new coordinate system. Moreover, instead of solving the problem (A.26) on the transformed domain, we choose a rectangular domain in the new coordinate system and after solving the problem we transform back the resulting solution into the original coordinate system.*

#### Discretization Scheme

In this section we derive a stable 7-point discretization scheme for the transformed forward committor equation (A.26). The scheme for the transformed backward committor equation follows analogously. Again, the transformed principle part as well as the transformed drift field are discretized by standard schemes which are found in [44]. The key observation in the derivation of the scheme is that we can decompose the transformed drift field such that the M-matrix property of the resulting discretization matrix is achieved.

**Discretization of the principle part** Without loss of generality, the principle part of (A.25) can be written as

$$\mathbf{a} : \nabla \nabla q = c^2 \gamma \beta^{-1} (\Delta q - 2 \frac{\partial^2 q}{\partial \eta \partial \xi}). \quad (\text{A.29})$$

In contrast to the elliptic case, here we additionally have to deal with a mixed-derivative part. The discretization is done by utilizing again a standard scheme (see

## A. Appendix

[44], page 91). Unlike to the elliptic case, here it is necessary that the mesh  $\Omega_h$  is total uniform, i.e.

$$h_\eta = h_\xi \stackrel{def}{=} h, \quad (\text{A.30})$$

where  $h_\eta$  is the mesh width of  $\Omega_h$  in  $\eta$ -direction and  $h_\xi$  the mesh width in  $\eta$ -direction. Doing so, we have

$$\frac{\partial^2}{\partial \eta \partial \xi} \rightsquigarrow \frac{1}{2} h^{-2} \begin{pmatrix} 1 & -1 & 0 \\ -1 & 2 & -1 \\ 0 & -1 & 1 \end{pmatrix}.$$

Together with the 5-point stencil for the Laplace operator (cf. (A.8)) we end up with a 3-point stencil for the principle part:

$$c^2 \gamma \beta^{-1} (\Delta - 2 \frac{\partial^2}{\partial \eta \partial \xi}) \rightsquigarrow c^2 \gamma \beta^{-1} h^{-2} \begin{pmatrix} 1 & 0 & 0 \\ 0 & -2 & 0 \\ 0 & 0 & 1 \end{pmatrix}. \quad (\text{A.31})$$

**Discretization of the drift part** In order to ensure invertibility of the final discretization matrix  $\mathbf{L}_h$  we decompose the transformed drift field  $\mathbf{b}(\eta, \xi) = \mathbf{b}^1(\eta, \xi) + \mathbf{b}^2(\eta, \xi) + \mathbf{b}^3(\eta, \xi)$  according to

$$\mathbf{b}(\eta, \xi) = \underbrace{\frac{\xi - \eta}{2} \begin{pmatrix} 0 \\ 1 \end{pmatrix}}_{=\mathbf{b}^1(\eta, \xi)} + \underbrace{\frac{\xi - \eta}{2} \begin{pmatrix} 1 + \gamma \\ -\gamma \end{pmatrix}}_{=\mathbf{b}^2(\eta, \xi)} + c \underbrace{\begin{pmatrix} \nabla_x V(c(\eta + \xi)) \\ -\nabla_x V(c(\eta + \xi)) \end{pmatrix}}_{=\mathbf{b}^3(\eta, \xi)} \quad (\text{A.32})$$

and separately discretize the vector fields  $\mathbf{b}^1$ ,  $\mathbf{b}^2$  and  $\mathbf{b}^3$  by means of the first-order standard stencil

$$h^{-1} \begin{bmatrix} 0 & b_{i2}^+ & 0 \\ -b_{i1}^- & -|b_1^i| - |b_2^i| & b_{i1}^+ \\ 0 & -b_{i2}^- & 0 \end{bmatrix},$$

where we set  $b_{ij}^+ = \max\{\mathbf{b}_j^i, 0\}$ ,  $b_{ij}^- = \min\{\mathbf{b}_j^i, 0\}$  and  $\mathbf{b}_j^i$  is the  $j^{\text{th}}$  component of the drift field  $\mathbf{b}^i = (\mathbf{b}_1^i, \mathbf{b}_2^i)^T$  evaluated in a mesh point. Combining the resulting three stencils in one, we end up with a 5-point stencil for the drift part

$$h^{-1} \begin{pmatrix} 0 & b_{12}^+ + b_{22}^+ + b_{32}^+ & 0 \\ -b_{11}^- - b_{21}^- - b_{31}^- & -[\sum_{i=1}^3 \sum_{j=1}^2 |\mathbf{b}_j^i|] & b_{11}^+ + b_{21}^+ + b_{31}^+ \\ 0 & -b_{12}^- - b_{22}^- - b_{32}^- & 0 \end{pmatrix}. \quad (\text{A.33})$$

**Discretization of the Neumann-like boundary conditions** We exemplify the derivation of the Neumann-like boundary condition (A.2) in a mesh point on the right boundary. Let  $\mathbf{x} = (\eta, \xi) \in \partial\Omega_h$  be a mesh point on the right boundary and  $\hat{\mathbf{n}} = (1, 0)^T$  the corresponding unit normal vector. The boundary condition (A.2) reduces to

$$0 = \nabla u(\mathbf{x}) \cdot \mathbf{a} \hat{\mathbf{n}} = \frac{\partial u(\mathbf{x})}{\partial \eta} - \frac{\partial u(\mathbf{x})}{\partial \xi}$$

which is consistently discretized by the scheme

$$0 = h^{-1}[u(\eta - h, \xi) - u(\eta, \xi)] + h^{-1}[u(\eta, \xi) - u(\eta, \xi + h)].$$

### A.1. Discretization of the Committor Equation

The derivation of the schemes for the left, upper and lower boundary are analogously. Eventually, we end up with the following stencils for the right and left boundary

$$h^{-1} \begin{bmatrix} 0 & 1 & 0 \\ 1 & -2 & 0 \\ 0 & 0 & 0 \end{bmatrix}, h^{-1} \begin{bmatrix} 0 & 0 & 0 \\ 0 & -2 & 1 \\ 0 & 1 & 0 \end{bmatrix} \quad (\text{A.34})$$

and for the lower and upper boundary

$$h^{-1} \begin{bmatrix} 0 & 1 & 0 \\ 1 & -2 & 0 \\ 0 & 0 & 0 \end{bmatrix}, h^{-1} \begin{bmatrix} 0 & 0 & 0 \\ 0 & -2 & 1 \\ 0 & 1 & 0 \end{bmatrix}. \quad (\text{A.35})$$

Finally, we state the discretization stencils for the corners. Since the mesh is total uniform, we can simply use the following stencils for the top-left and the bottom-right corner:

$$h^{-1} \begin{bmatrix} 0 & 0 & 0 \\ 0 & -1 & 0 \\ 0 & 0 & 1 \end{bmatrix}, h^{-1} \begin{bmatrix} 1 & 0 & 0 \\ 0 & -1 & 0 \\ 0 & 0 & 0 \end{bmatrix}. \quad (\text{A.36})$$

Unfortunately, we cannot simply apply one of the above schemes in the bottom-left and top right corner of the rectangular mesh  $\Omega_h$  but the boundary condition (A.2) in a corner  $\mathbf{x}_c \in \Omega_h$  is in particular satisfied if

$$0 = \frac{\partial u(\mathbf{x}_c)}{\partial \eta} = \frac{\partial u(\mathbf{x}_c)}{\partial \xi}.$$

The stencils for these relaxed boundary conditions in the bottom-left and top-right corner then take the form

$$h^{-1} \begin{bmatrix} 0 & 1 & 0 \\ 0 & -2 & 1 \\ 0 & 0 & 0 \end{bmatrix}, h^{-1} \begin{bmatrix} 0 & 0 & 0 \\ 1 & -2 & 0 \\ 0 & 1 & 0 \end{bmatrix}. \quad (\text{A.37})$$

**Discretization matrix** Like in the elliptic case, we discretize the operator  $\mathfrak{L}_{\mathbf{bw}}$  on  $\overline{\Omega}_h^S$  in  $\overline{\Omega}_h^S$  (cf. Sect. A.1.1) and denote the resulting discretization matrix by  $D_h$ . The combination of  $D_h$  with the matrix  $N_h$  which results from the explicit discretization of Neumann conditions is denoted by  $\overline{D}_h$ . Finally, the elimination of the Dirichlet condition leads to the matrix  $\overline{L}_h$ .

**M-matrix property** In this section it is convenient to use the notation introduced in Section A.6. In the elliptic case, the irreducibility of the matrix  $\overline{L}_h$  is a direct consequence of the symmetry of the discretization stencils (cf. (A.8)). Here, the irreducibility of  $\overline{L}_h$  follows from the special decomposition of the transformed vector field in (A.32).

For the sake of a compact notation, we define for a mesh point  $\mathbf{z} = (z_1, z_2) \in \Omega_h$  a *diagonal* by

$$\mathcal{D}_{\mathbf{z}} = \overline{\Omega}_h \cap \left\{ \mathbf{z} + \alpha \begin{pmatrix} -1 \\ 1 \end{pmatrix} : \alpha \in \mathbb{R} \right\}.$$

## A. Appendix

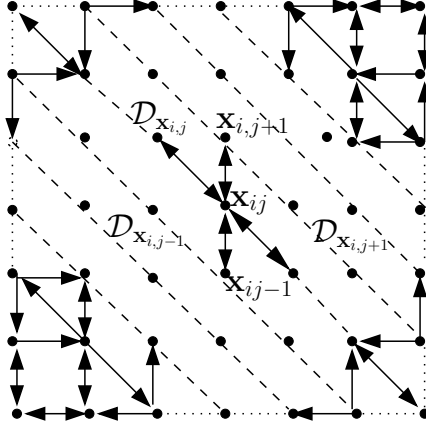


Figure A.3.: Schematic representation of the graph induced by the discretization stencils in (A.31), (A.33) and in (A.34)-(A.37). The diffusion stencil (A.31) ensures the connection of all mesh points lying on the same diagonal whereas the connection among diagonals in the direct vicinity is guaranteed by the stencil in (A.33) via Lemma A.1.4.

A first observation is that the diffusion stencil (A.31) guarantees the mutually connection of all mesh points lying on the same diagonal.

Furthermore, we can prove that diagonals in the direct vicinity to each other are connected too.

**Lemma A.1.4.** *Let  $\mathbf{x}_{i,j} = (\eta_0 + ih, \xi_0 + jh) \in \overline{\Omega}_h^S$  be a mesh point. Then the diagonal  $\mathcal{D}_{\mathbf{x}_{i,j}}$  is connected at least with one of the diagonals  $\mathcal{D}_{\mathbf{x}_{i,j+1}}$  and  $\mathcal{D}_{\mathbf{x}_{i,j-1}}$ . If  $\mathbf{x}_{i,j} \in \Omega_h^S$  then  $\mathcal{D}_{\mathbf{x}_{i,j}}$  is connected with both.*

*Proof.* Let  $\mathbf{x}_{i,j} \in \Omega_h$  and, firstly, assume that neither  $\mathbf{x}_{i,j+1}$  nor  $\mathbf{x}_{i,j-1}$  lies on the boundary  $\partial\Omega_h$  and that  $\eta_i \neq \xi_j$ . Consider the vector field decomposition in (A.32) and the stencil given in (A.33); provided that  $\gamma > 0$  we deduce

$$\mathbf{b}_{12} \neq 0 \Leftrightarrow -\gamma \frac{\eta_i - \xi_j}{2} \neq 0 \Leftrightarrow \mathbf{b}_{22} \neq 0.$$

But this immediately implies that either

$$\mathbf{b}_{12}^+ \neq 0 \text{ and } \mathbf{b}_{22}^- \neq 0 \quad \text{or} \quad \mathbf{b}_{12}^- \neq 0 \text{ and } \mathbf{b}_{22}^+ \neq 0$$

holds true and, hence,  $\mathbf{x}_{i,j}$  is directly connected with  $\mathbf{x}_{i,j-1}$  and  $\mathbf{x}_{i,j+1}$ , respectively.

Next, let  $\mathbf{x}_{i,j} \in \partial\Omega_h$ . The stencils in (A.34) and (A.34) for the discretization of the Neumann-like condition show that  $\mathbf{x}_{i,j}$  is directly connected to a mesh point in  $\Omega_h$  and hence  $\mathcal{D}_{\mathbf{x}_{i,j}}$  is connected at least with one of the diagonals  $\mathcal{D}_{\mathbf{x}_{i,j+1}}$  and  $\mathcal{D}_{\mathbf{x}_{i,j-1}}$ . The same reasoning holds true for the corners.  $\square$

For a schematic representation of the connectivity of diagonals induced by the discretization matrix  $\overline{L}_h$  see Figure A.3. Now we are prepared to prove

**Lemma A.1.5.** *The matrix  $-\overline{L}_h$  is an M-matrix.*

## A.2. Weak Formulation for the Elliptic Mixed-Boundary Value Problem

*Proof.* The matrix  $-\bar{L}_h$  satisfies the sign conditions (A.60) and (A.61) and for every mesh point in the direct vicinity of  $\partial A_h \cup \partial B_h$  we have

$$|\bar{L}_h(\mathbf{x}, \mathbf{x})| > \sum_{\mathbf{y} \neq \mathbf{x}} |\bar{L}_h(\mathbf{x}, \mathbf{y})|. \quad (\text{A.38})$$

But from the connectivity within the diagonals, by Lemma A.1.4 and the discretization of the Neumann-like boundary conditions it immediately follows that for every mesh point  $\mathbf{z} \in \bar{\Omega}_h^S$  we can find a directed path  $p = (\mathbf{z} = \mathbf{x}_0, \dots, \mathbf{x}_n), \mathbf{x}_0, \dots, \mathbf{x}_n \in \bar{\Omega}_h^S$  in the graph associated with  $\bar{L}_h$  to an  $\mathbf{x}_n$  which satisfies the inequality in (A.38). For schematic presentation of the associated graph see Figure A.3. This proves that  $-\bar{L}_h$  is essentially diagonally dominant and, finally, by virtue of Theorem A.6.6 we are done.  $\square$

### Stability and Convergence

The proof that the discretization scheme for the Langevin committor equation is stable as well as the proof of convergence is analogously to the proof for the Smoluchowski case, given in Section A.1.2 and Section A.1.2 because we only exploited the M-matrix property of the discretization matrix and the consistency of the schemes.

We summarize both results in

**Theorem A.1.3.** *The discretization scheme resulting from (A.31), (A.33) together with the stencils in (A.34)-(A.37) is stable. The stability constant is given by*

$$C = 2 \max_{\mathbf{x} \in \bar{\Omega} \setminus \mathcal{S}} \{|s(\mathbf{x})|\},$$

where the function  $s(x) \in C^2(\Omega) \cap C^1(\bar{\Omega})$  is the solution of the auxiliary mixed-boundary value problem

$$\begin{cases} \mathfrak{L}_{bw} s = -1 & \text{in } \Omega \setminus \mathcal{S} \\ s = 0 & \text{on } \partial \mathcal{S} \\ \nabla s \cdot \mathbf{a}\hat{\mathbf{n}} = -1 & \text{on } \partial \Omega. \end{cases} \quad (\text{A.39})$$

Let  $u$  be the analytical solution of the mixed-boundary value problem (A.26) and let  $\bar{u}_h = \bar{L}_h^{-1} \bar{F}_h$  denote the approximated solution with respect to the total uniform mesh width  $h$ . Then we have

$$\lim_{h \rightarrow 0} \left\| \bar{u}_h - \bar{R}_h^S u \right\|_{\infty} = 0.$$

## A.2. Weak Formulation for the Elliptic Mixed-Boundary Value Problem

In this section we will derive a weak formulation of the elliptic mixed-boundary value problem

$$\begin{cases} \beta^{-1} \Delta u + \nabla V \cdot \nabla u = f & \text{in } \Omega_S \stackrel{\text{def}}{=} \Omega \setminus \mathcal{S} \\ u = g_D & \text{on } \partial \mathcal{S} \\ \frac{\partial u}{\partial \hat{\mathbf{n}}} = g_N & \text{on } \partial \Omega \end{cases} \quad (\text{A.40})$$

A. Appendix

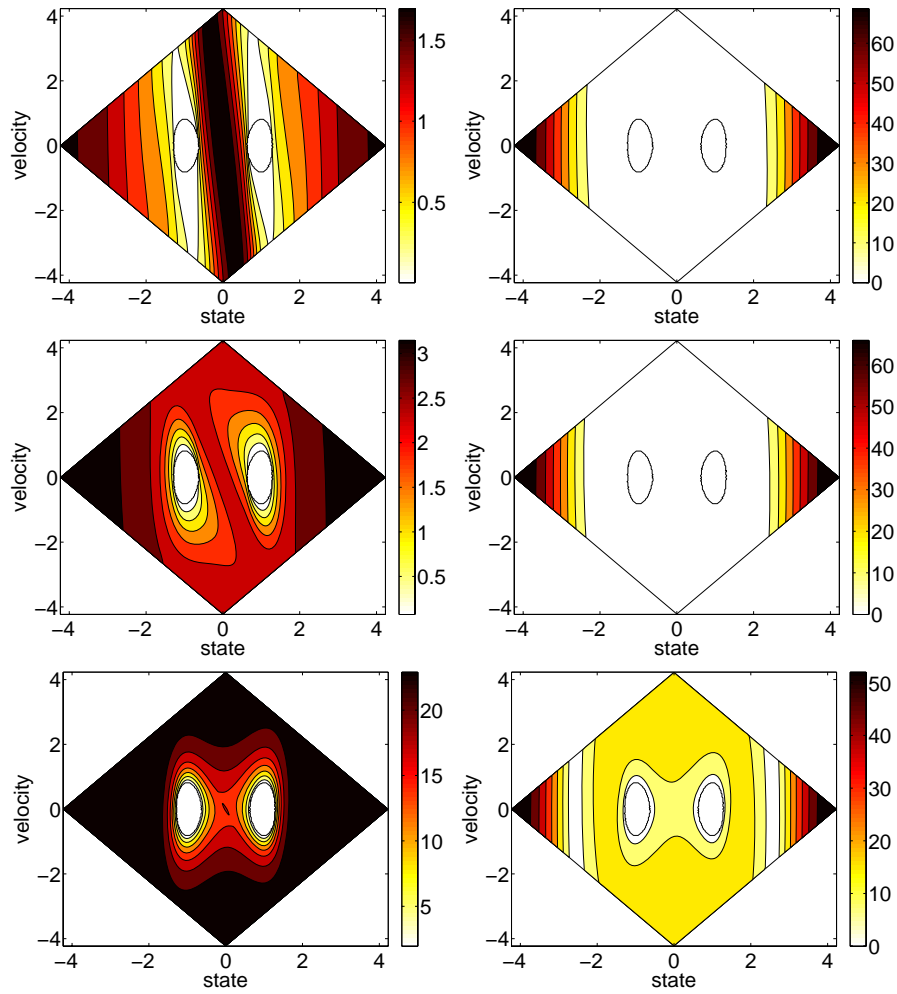


Figure A.4.: Contour plots of solutions of the mean first passage times equation (3.10) with respect to the set  $\mathcal{S} = A \cup B$  (first column) and solutions  $|s(x)|$  of the auxiliary problem in (A.39) (second column). Results for constant temperature  $\beta = 1$  and for three different friction constants: from top to bottom:  $\gamma = 10$ ,  $\gamma = 1$  and  $\gamma = 0.001$ .



## A.2. Weak Formulation for the Elliptic Mixed-Boundary Value Problem

where  $\Omega \subset \mathbb{R}^d$  is a domain (open and connected) and  $\mathcal{S} \subset \Omega$  is a close subset. In particular, we show the existence of a weak solution of the problem (A.7) and (A.16). For the derivation we follow the usual steps, except that we introduce a suitable weight function which simplifies the resulting bilinear form in the weak formulation.

As the weight function, we choose the equilibrium probability density function of the Smoluchowski dynamics (2.37), that is

$$\alpha(x) \stackrel{def}{=} \exp(-\beta V(x)),$$

where  $\beta > 0$  is usually referred to as the inverse temperature. Provided that the potential  $V(x)$  is sufficiently smooth, we have

$$0 < \alpha_0 \leq \alpha(x) \leq \alpha_1 < \infty, \quad \forall x \in \overline{\Omega_{\mathcal{S}}},$$

where we set  $\alpha_0 = \min_{x \in \overline{\Omega_{\mathcal{S}}}} \{\alpha(x)\}$  and  $\alpha_1 = \max_{x \in \overline{\Omega_{\mathcal{S}}}} \{\alpha(x)\}$ . For a compact notation we abbreviate the inner product on  $L^2(\Omega_{\mathcal{S}})$  by

$$(u, v) \stackrel{def}{=} \int_{\Omega_{\mathcal{S}}} u(x)v(x) dx.$$

In the first step of the derivation of the weak formulation we multiply the equation in (A.40) with a test function  $\phi \in C^\infty(\Omega_{\mathcal{S}})$  and with the weight function  $\alpha(x)$ . Integrating over the domain  $\Omega_{\mathcal{S}}$  yields

$$\beta^{-1}(\Delta u, \phi\alpha) - (\nabla V, \nabla u \phi\alpha) = (f, \phi\alpha). \quad (\text{A.41})$$

By Green's first integral identity and  $\nabla\alpha = -\beta\nabla V\alpha$  we expand the first integral in the equation (A.41)

$$\begin{aligned} \beta^{-1}(\Delta u, \phi\alpha) &= (\nabla V, \nabla u \phi\alpha) - \beta^{-1}(\nabla u, \nabla\phi\alpha) \\ &+ \beta^{-1} \int_{\partial\mathcal{S}} \frac{\partial u}{\partial \hat{n}} \phi\alpha d\sigma_{\partial\mathcal{S}}(x) + \beta^{-1} \int_{\partial\Omega} \frac{\partial u}{\partial \hat{n}} \phi\alpha d\sigma_{\partial\Omega}(x). \end{aligned} \quad (\text{A.42})$$

Substituting the left hand side of (A.42) in (A.41) and recalling that the normal derivative is prescribed on  $\partial\Omega$  we end up with

$$(\nabla u, \nabla\phi\alpha) - \int_{\partial\mathcal{S}} \frac{\partial u}{\partial \hat{n}} \phi\alpha d\sigma_{\partial\mathcal{S}}(x) - \int_{\partial\Omega} g_N \phi\alpha d\sigma_{\partial\Omega}(x) = -\beta(f, \phi\alpha).$$

The last equation motivates the following weak formulation

$$\begin{aligned} &\text{Find } u \in H^1(\Omega_{\mathcal{S}}) \text{ such that} \\ &\begin{cases} a(u, \phi) = l_{f, g_N}(\phi), & \forall \phi \in H^1(\Omega_{\mathcal{S}}) \\ u = g_D \text{ on } \partial\mathcal{S} \end{cases} \end{aligned} \quad (\text{A.43})$$

where we define

$$a(u, \phi) \stackrel{def}{=} (\nabla u, \nabla\phi\alpha), \quad (\text{A.44})$$

$$l_{f, g_N}(\phi) \stackrel{def}{=} -\beta(f, \phi\alpha) + \int_{\partial\Omega} g_N \phi\alpha d\sigma_{\partial\Omega}(x). \quad (\text{A.45})$$

## A. Appendix

Notice that the function  $a(\cdot, \cdot)$  is a symmetric bilinear form and the function  $l_{f, g_N}(\cdot)$  is linear. Provided that the function  $g_D \in H^{\frac{1}{2}}(\partial S)$  we can use its continuation  $\bar{g}_D(x)$  to decompose the unknown function  $u(x)$  by  $u(x) = w(x) + \bar{g}_D(x)$ , where the new unknown function  $w(x)$  has to vanish on  $\partial S$ . This leads to an equivalent weak formulation

$$\begin{aligned} &\text{Find } w \in \mathcal{H} \text{ such that} \\ &a(w, \phi) = l_{f, g_N}(\phi) - a(\bar{g}_D, \phi), \quad \forall \phi \in H^1(\Omega_S) \end{aligned} \quad (\text{A.46})$$

where the Sobolev space  $\mathcal{H}$  is defined by

$$\mathcal{H} \stackrel{\text{def}}{=} \{v \in H^1(\Omega_S) : tr_{\partial S} v = 0\}. \quad (\text{A.47})$$

### A.2.1. Existence of a Weak Solution

The existence of a unique solution of the weak problem (A.46) is usually proved by showing that the prerequisites of the Lemma of Lax-Milgram are satisfied. In doing so, we have to show that the bilinear form (A.44) is  $\mathcal{H}$ -elliptic, i.e.,

$$\exists c_1 > 0 : \quad a(v, v) \geq c_1 \|v\|_{H^1}^2 \quad \forall v \in \mathcal{H} \quad (\text{A.48})$$

$$\exists c_2 > 0 : \quad |a(v, w)| \leq c_2 \|v\|_{H^1} \|w\|_{H^1} \quad \forall v, w \in \mathcal{H} \quad (\text{A.49})$$

and that the linear function defined on the right hand side of (A.46) is an element in the dual space  $(H^1(\Omega_S))' = \{l : H^1(\Omega_S) \rightarrow \mathbb{R} : l \text{ is linear and continuous}\}$ .

We first prove that our bilinear form (A.44) satisfies the condition (A.48). Let  $v \in C^\infty(\overline{\Omega_S})$  such that  $v|_{\partial S} = 0$ . Then we deduce

$$a(v, v) = \int_{\Omega_S} \nabla v \cdot \nabla v \alpha \, dx \geq \alpha_0 \|\nabla v\|_{L^2}^2.$$

In the last step we estimate the  $H^1$ -norm of  $v$  by

$$\begin{aligned} \alpha_0 \|v\|_{H^1}^2 &= \alpha_0 \left( \|v\|_{L^2}^2 + \|\nabla v\|_{L^2}^2 \right) \\ &\leq \alpha_0 \left( C \|\nabla v\|_{L^2}^2 + \|\nabla v\|_{L^2}^2 \right) \\ &\leq (1 + C) a(v, v), \end{aligned}$$

where the first inequality follows from the Poincaré-inequality for functions vanishing only on a part of the boundary (see Theorem A.6.3 in Appendix). Since  $C^\infty(\overline{\Omega_S})$  is dense in  $H^1(\Omega_S)$  we get for  $0 < c_1 = (1 + C)/\alpha_0$  the desired result. The second condition (A.49) is a simple consequence of the Cauchy-Schwartz-inequality in  $\mathbb{R}^2$  and in  $L^2$ . We deduce

$$\begin{aligned} |a(v, w)| &\leq \alpha_1 \int_{\Omega_S} |\nabla v \cdot \nabla w| \, dx \\ &\leq \alpha_1 \int_{\Omega_S} |\nabla v| \cdot |\nabla w| \, dx \\ &\leq \alpha_1 \left( \int_{\Omega_S} |\nabla v|^2 \right)^{\frac{1}{2}} \cdot \left( \int_{\Omega_S} |\nabla w|^2 \right)^{\frac{1}{2}} \\ &\leq \alpha_1 \|v\|_{H^1} \|w\|_{H^1} \end{aligned}$$

## A.2. Weak Formulation for the Elliptic Mixed-Boundary Value Problem

In the last step we have to show that the right hand side in (A.46)

$$l_{f,g_N,g_D}(v) \stackrel{\text{def}}{=} -\beta^{-1}(f, \alpha v) + \int_{\partial\Omega} g_N \alpha v \, d\sigma_{\partial\Omega}(x) - a(\bar{g}_D, v)$$

belongs to  $(H^1(\Omega_S))'$ . Hence, we have to show that

$$\exists K > 0 : \|l_{f,g_N,g_D}\|_{(H^1)'} = \sup_{\|v\|_{H^1}=1} |l_{f,g_N,g_D}(v)| \leq K.$$

which immediately follows from

- 1.)  $|(f, \alpha v)| \leq \|f\alpha\|_{L^2} \cdot \|v\|_{H^1},$
- 2.)  $|a(\bar{g}_D, v)| \leq \alpha_1 \|\bar{g}_D\|_{H^1} \|v\|_{H^1},$
- 3.)  $|\int_{\partial\Omega} g_N \alpha v \, d\sigma_{\partial\Omega}(x)| \leq \|g_N \alpha\|_{L^2(\partial\Omega)} \cdot \|v\|_{H^1}.$

### A.2.2. Classical Solution vs. Weak Solution

The following theorem gives an answer to the question under which conditions a weak solution is also a classical solution.

**Theorem A.2.1.** *Let  $u \in C^2(\overline{\Omega_S}) \cap H^1(\Omega_S)$  be a solution of the weak problem (A.43). Then  $u$  is a classical solution, i.e.  $u \in C^2(\Omega_S) \cap C^1(\overline{\Omega_S})$ , of the mixed-boundary value problem (A.3).*

*Proof.* First notice that we have the following sequence of inclusions

$$H_0^1(\Omega_S) \subset \mathcal{H} \subset H^1(\Omega_S),$$

where  $\mathcal{H}$  is the Sobolev space defined in (A.47). Since  $u$  is a solution of the weak problem (A.43),

$$-\beta^{-1}(\nabla u, \nabla \phi \alpha) + \beta^{-1} \int_{\partial\Omega} g_N \phi \alpha \, d\sigma_{\partial\Omega}(x) = (f, \phi \alpha) \quad \forall \phi \in \mathcal{H},$$

we get by applying Green's integral identity

$$(\beta^{-1} \Delta u - \nabla V \nabla u, \phi \alpha) + \beta^{-1} \int_{\partial\Omega} (g_N - \frac{\partial u}{\partial \hat{n}}) \phi \alpha \, d\sigma_{\partial\Omega}(x) = (f, \phi \alpha) \quad \forall \phi \in \mathcal{H}$$

and in particular

$$((\beta^{-1} \Delta u - \nabla V \nabla u - f) \alpha, \phi) = 0 \quad \forall \phi \in H_0^1(\Omega_S).$$

Because of the strict positivity of the weight function  $\alpha(x)$  we conclude

$$\beta^{-1} \Delta u - \nabla V \nabla u = f \quad \text{in } \Omega_S.$$

Moreover, we obtain

$$\int_{\partial\Omega} (g_N - \frac{\partial u}{\partial \hat{n}}) \phi \alpha \, d\sigma_{\partial\Omega}(x) = 0 \quad \forall \phi \in H^1(\Omega_S)$$

which shows that the Neumann boundary conditions are also satisfied,

$$\frac{\partial}{\partial \hat{n}} u = g_N \quad \text{on } \partial\Omega.$$

By assumption, the function  $u$  satisfies the Dirichlet boundary conditions on  $\partial\mathcal{S}$  which completes the proof.  $\square$

### A.3. Approximation of Diffusion Processes via Markov Jump Processes

In this section we will show that the Birth-Death process in Section 4.3.1, given by its generator (4.44), is indeed an approximation of the considered Smoluchowski dynamics.

It is a well-known fact that every diffusion process of the form (2.8) can be approximated under weak conditions on the diffusion matrix by a Birth-Death process. In general, the opposite implication does not hold. According to Gardiner [41], Sect. 7.2, the basic idea of the proof that a family of Birth-Death processes, parameterized by a scaling parameter  $\epsilon$ , approximates a diffusion process is to show that in the limit  $\epsilon \rightarrow 0$  the associated Master-equations passes to the Fokker-Planck equation associated with the diffusion process. In order to explain that idea in more detail and to motivate our alternative approach, we present the construction given in [41], page 248. Consider a 1-dimensional diffusion process  $X_t \in \mathbb{R}$  of the form

$$dX_t = A(X_t)dt + \sqrt{B(X_t)}dW_t \quad (\text{A.50})$$

with sufficiently smooth coefficients  $A : \mathbb{R} \rightarrow \mathbb{R}$  and  $B : \mathbb{R} \rightarrow \mathbb{R}^+$ . The jump rates of the approximating Birth-Death process on the state space  $S = \epsilon\mathbb{Z}$  are defined according to

$$W_\epsilon(x, x') \stackrel{\text{def}}{=} \left( \frac{A(x)}{2\epsilon} + \frac{B(x)}{2\epsilon^2} \right) \delta_{x', x+\epsilon} + \left( -\frac{A(x)}{2\epsilon} + \frac{B(x)}{2\epsilon^2} \right) \delta_{x', x-\epsilon} \quad (\text{A.51})$$

such that for a sufficiently small  $\epsilon > 0$ , (A.51) is positive for all  $x \in S$ . Next it is shown, that in the limit  $\epsilon \rightarrow 0$ , the Master-equation

$$\begin{aligned} \frac{\partial p_\epsilon(x, t)}{\partial t} &= \int_{\mathbb{R}} [W_\epsilon(x', x)p_\epsilon(x', t) - W_\epsilon(x, x')p_\epsilon(x, t)] dx' \\ &= W_\epsilon(x - \epsilon, x)p(x - \epsilon, t) + W_\epsilon(x + \epsilon, x)p_\epsilon(x + \epsilon, t) \\ &\quad - (W_\epsilon(x, x + \epsilon) + W_\epsilon(x, x - \epsilon))p_\epsilon(x, t) \end{aligned} \quad (\text{A.52})$$

becomes the Fokker-Planck equation

$$\frac{\partial p(x, t)}{\partial t} = \mathcal{L}_{fw}p(x, t) = \frac{1}{2} \frac{\partial^2}{\partial x^2} (B(x)p(x, t)) - \frac{\partial}{\partial x} (A(x)p(x, t)). \quad (\text{A.53})$$

An alternative way to see that the Master-equation passes in the limit  $\epsilon \rightarrow 0$  to (A.53) bases on the observation that from the view point of finite differences, the right hand side in (A.51) results from a second order finite differences discretization of the operator

$$\mathcal{L}_{bw} = \frac{1}{2} B(x) \frac{\partial^2}{\partial x^2} + A(x) \frac{\partial}{\partial x},$$

which is the generator associated with the diffusion process in (A.50). For the sake of simplicity we consider the diffusion process of a finite interval  $[a, b] \subset \mathbb{R}$  and assume periodic boundary conditions. Let  $W_\epsilon \in \mathbb{R}^{|S| \times |S|}$  denote the matrix resulting from the jump rates in (A.51) where  $S = \epsilon\mathbb{Z} \cap [a, b]$  and we additionally set

$$W_\epsilon(x, x) \stackrel{\text{def}}{=} -(W_\epsilon(x, x + \epsilon) + W_\epsilon(x, x - \epsilon)).$$

Notice that the Master equation in (A.52) can now be written in a compact form,

$$\frac{\partial p_\epsilon}{\partial t} = W_\epsilon^T p_\epsilon,$$

where  $p_\epsilon = (p_\epsilon(x))_{x \in S}$ . Encouraged by a Remark in [44], page 94, we next show that the transposed matrix  $W_\epsilon^T$  is a consistent discretization of the operator  $\mathcal{L}_{fw}$  on the right hand side in the Fokker-Planck equation (A.53). With the notation introduced in Section A.1, we have for any  $p \in C^2$

**Lemma A.3.1.**

$$\|W_\epsilon^T R_\epsilon p - R_\epsilon \mathcal{L}_{fw} p\|_\infty \rightarrow 0 \text{ as } \epsilon \rightarrow 0.$$

*Proof.* Let  $x \in S$  be a mesh point. We deduce

$$\begin{aligned} (W_\epsilon^T R_\epsilon p)(x) &= W_\epsilon(x - \epsilon, x)p(x - \epsilon) + W_\epsilon(x + \epsilon, x)p(x + \epsilon) \\ &\quad - (W_\epsilon(x, x + \epsilon) + W_\epsilon(x, x - \epsilon))p(x) \\ &= \frac{1}{2\epsilon^2} [B(x - \epsilon)p(x - \epsilon) - B(x)p(x) + 2B(x + \epsilon)p(x + \epsilon)] \\ &\quad - \frac{1}{2\epsilon} [A(x + \epsilon)p(x + \epsilon) - A(x - \epsilon)p(x - \epsilon)] \\ &= \frac{1}{2} \frac{\partial^2}{\partial x^2} (B(x)p(x)) + \mathcal{O}(\epsilon^2) - \frac{\partial}{\partial x} (A(x)p(x)) + \mathcal{O}(\epsilon^2), \end{aligned}$$

which proves the assertion.  $\square$

The view point that the construction of the jump rates of an approximating Birth-Death process can also be obtained via finite difference discretization of the generator  $\mathcal{L}_{bw}$  allows a straightforward generalization for the approximation of diffusion processes in higher dimension. For example, the generator of the Birth-Death process considered in Section 4.3.1, results from the discretization of the generator

$$\mathcal{L}_{bw} = \beta^{-1} \Delta - \nabla V \nabla$$

via the second order scheme in (A.8) where we additionally included reflecting boundary conditions.

## A.4. Proofs

### A.4.1. Proof for the Representation of the Probability Current of Reactive Trajectories

To derive (3.15), we take first the limit as  $T \rightarrow \infty$  in (3.14) using ergodicity to obtain

$$\begin{aligned} \lim_{s \rightarrow 0^+} \frac{1}{s} &\left( \int_S \rho(x) q_b(x) \mathbb{E}_x(q(X(s)) \mathbf{1}_{\mathbb{R}^d \setminus S}(X(s))) dx \right. \\ &\quad \left. - \int_{\mathbb{R}^d \setminus S} \rho(x) q_b(x) \mathbb{E}_x(q(X(s)) \mathbf{1}_S(X(s))) dx \right) \\ &= \int_{\partial S} \hat{n}_{\partial S}(x) \cdot J_{AB}(x) d\sigma_{\partial S}(x), \end{aligned} \quad (\text{A.54})$$

## A. Appendix

where  $\mathbb{E}_x$  denotes expectation conditional on  $X(0) = x$ . Taking the limit as  $s \rightarrow 0^+$  can now be done using

$$\begin{aligned} & \lim_{t \rightarrow 0^+} \frac{1}{t} (\mathbb{E}_x \phi(X(t)) - \phi(x)) \\ &= \sum_{i,j=1}^d a_{ij}(x) \frac{\partial^2 \phi(x)}{\partial x_i \partial x_j} + \sum_{i=1}^d b_i(x) \frac{\partial \phi(x)}{\partial x_i} \equiv (\mathcal{L}_{bw} \phi)(x), \end{aligned}$$

where  $\phi(x)$  is any suitable observable. However, taking the limit on (A.54) is somewhat tricky because of the presence of the discontinuous functions  $\mathbf{1}_{\mathcal{S}}(x)$  and  $\mathbf{1}_{\mathbb{R}^d \setminus \mathcal{S}}(x)$ . The proper way to avoid ambiguities on how to interpret the derivatives of  $\mathbf{1}_{\mathcal{S}}(x)$  and  $\mathbf{1}_{\mathbb{R}^d \setminus \mathcal{S}}(x)$  is to mollify these functions, that is, replace them by functions varying rapidly on  $\partial \mathcal{S}$  but smooth, then let  $s \rightarrow 0^+$  and finally remove the mollification. Let then  $f_\delta(x)$  be a smooth function which is 1 in  $\mathcal{S}$  at a distance  $\delta$  from  $\partial \mathcal{S}$ , 0 out of  $\mathcal{S}$  at a distance  $\delta$  from  $\partial \mathcal{S}$  and varies rapidly but smoothly from 0 to 1 in the strip of size  $2\delta$  around  $\partial \mathcal{S}$ . Thus (A.54) is the limit as  $\delta \rightarrow 0$  of

$$\begin{aligned} I_\delta &= \lim_{s \rightarrow 0^+} \frac{1}{s} \int_{\mathbb{R}^d} \rho(x) q_b(x) \\ &\quad \times \left( f_\delta(x) \mathbb{E}_x(q(X(s))(1 - f_\delta(X(s)))) - \right. \\ &\quad \left. (1 - f_\delta(x)) \mathbb{E}_x(q(X(s))f_\delta(X(s))) \right) dx. \end{aligned}$$

Inserting

$$\begin{aligned} 0 &= -\rho(x) q_b(x) f_\delta(x) (q(x)(1 - f_\delta(x))) \\ &\quad + \rho(x) q_b(x) (1 - f_\delta(x)) (q(x) f_\delta(x)) \end{aligned}$$

under the integral then letting  $s \rightarrow 0^+$ , we obtain

$$\begin{aligned} I_\delta &= \int_{\mathbb{R}^d} \rho(x) q_b(x) \left( f_\delta(x) (\mathcal{L}_{bw}(q(1 - f_\delta)))(x) \right. \\ &\quad \left. - (1 - f_\delta(x)) (\mathcal{L}_{bw}(q f_\delta))(x) \right) dx. \end{aligned}$$

Expanding the integrand, several terms cancel and we are simply left with

$$I_\delta = - \int_{\mathbb{R}^d} \rho(x) q_b(x) (\mathcal{L}_{bw}(q f_\delta))(x) dx.$$

Using the explicit form for  $L$  and expanding, this is

$$\begin{aligned} I_\delta &= - \int_{\mathbb{R}^d} \rho(x) q_b(x) \left( f_\delta(x) \mathcal{L}_{bw} q(x) \right. \\ &\quad + \sum_{i,j=1}^d a_{ij}(x) \frac{\partial}{\partial x_i} \left( q(x) \frac{\partial f_\delta(x)}{\partial x_j} \right) \\ &\quad \left. + \sum_{i=1}^d \frac{\partial f_\delta(x)}{\partial x_i} \left( b_i(x) q(x) + \sum_{j=1}^d a_{ij}(x) \frac{\partial q(x)}{\partial x_j} \right) \right) dx. \end{aligned}$$

By (3.6),  $\mathcal{L}_{bw}q(x) = 0$  and integrating by parts the second term in the parenthesis under the integral, we arrive at

$$\begin{aligned} I_\delta &= - \int_{\mathbb{R}^d} \sum_{i=1}^d \frac{\partial f_\delta(x)}{\partial x_i} \left( q(x)q_b(x)J_i(x) \right. \\ &\quad \left. + q_b(x)\rho(x) \sum_{j=1}^d a_{ij}(x) \frac{\partial q(x)}{\partial x_j} \right. \\ &\quad \left. - q(x)\rho(x) \sum_{j=1}^d a_{ij}(x) \frac{\partial q_b(x)}{\partial x_j} \right) dx. \end{aligned}$$

Now let  $\delta \rightarrow 0$  and recall that for any suitable  $F(x) = (F_1(x), \dots, F_d(x))^T$

$$\begin{aligned} &\lim_{\delta \rightarrow 0} \int_{\mathbb{R}^d} \sum_{i=1}^d \frac{\partial f_\delta(x)}{\partial x_i} F_i(x) dx \\ &= - \lim_{\delta \rightarrow 0} \int_{\mathbb{R}^d} f_\delta(x) \sum_{i=1}^d \frac{\partial F_i(x)}{\partial x_i} dx \\ &= - \int_{\mathcal{S}} \sum_{i=1}^d \frac{\partial F_i(x)}{\partial x_i} dx \\ &= - \int_{\partial \mathcal{S}} \sum_{i=1}^d \hat{n}_{\mathcal{S},i}(x) F_i(x) d\sigma_{\partial \mathcal{S}}(x), \end{aligned}$$

where the first equality follows by integration by parts, the second by definition of  $f_\delta(x)$ , and the third by the divergence theorem. Using this result, we conclude that the limit of the expression above for  $I_\delta$  as  $\delta \rightarrow 0$  is the surface integral of the current  $J_{AB}(x)$  given in (3.15), as claimed.

#### A.4.2. Proof for the Representation of the Transition Rate via a Volume Integral

To check that (3.19) gives the rate, let  $\partial \mathcal{S}(\zeta) = \{x : q(x) = \zeta\}$  be the (forward) isocommittor surface with committor value  $\zeta \in [0, 1]$ , and consider the integral

$$A(\zeta) = \int_{\partial \mathcal{S}(\zeta)} \rho(x) \sum_{i,j=1}^d \hat{n}_{\partial \mathcal{S}(\zeta),i}(x) a_{ij}(x) \frac{\partial q(x)}{\partial x_j} d\sigma_{\partial \mathcal{S}(\zeta)}(x).$$

Since  $\partial \mathcal{S}(0) \equiv \partial A$ , is easy to see from (3.17) and (3.18) with  $\partial \mathcal{S} = \partial A$  that:

$$\begin{aligned} A(0) &= \int_{\partial A} \rho(x) \sum_{i,j=1}^d \hat{n}_{\partial A,i}(x) a_{ij}(x) \frac{\partial q(x)}{\partial x_j} d\sigma_{\partial A}(x) \\ &\equiv k_{AB}, \end{aligned}$$

where we used  $q(x) = 0$  and  $q_b(x) = 1$  on  $\partial A$ . Next, we show that  $A(\zeta) = A(0) = k_{AB}$  for all  $\zeta \in [0, 1]$ . Using the Dirac delta function we can express  $A(\zeta)$  as

$$A(\zeta) = \int_{\mathbb{R}^d} \rho(x) \sum_{i,j=1}^d \frac{\partial q(x)}{\partial x_i} a_{ij}(x) \frac{\partial q(x)}{\partial x_j} \delta(q(x) - \zeta) dx$$

## A. Appendix

and hence

$$\begin{aligned} & \frac{dA(\zeta)}{d\zeta} \\ &= - \int_{\mathbb{R}^d} \rho(x) \sum_{i,j=1}^d \frac{\partial q(x)}{\partial x_i} a_{ij}(x) \frac{\partial q(x)}{\partial x_j} \delta'(q(x) - \zeta) dx \\ &= - \int_{\mathbb{R}^d} \rho(x) \sum_{i,j=1}^d \frac{\partial q(x)}{\partial x_i} a_{ij}(x) \frac{\partial}{\partial x_j} \delta(q(x) - \zeta) dx. \end{aligned}$$

Integrating by parts, this gives

$$\begin{aligned} \frac{dA(\zeta)}{d\zeta} &= \int_{\mathbb{R}^d} \rho(x) \sum_{i,j=1}^d a_{ij}(x) \frac{\partial^2 q(x)}{\partial x_i \partial x_j} \delta(q(x) - \zeta) dx \\ &+ \int_{\mathbb{R}^d} \sum_{i,j=1}^d \frac{\partial q(x)}{\partial x_i} \frac{\partial}{\partial x_j} (a_{ij}(x) \rho(x)) \delta(q(x) - \zeta) dx \\ &= - \int_{\mathbb{R}^d} \rho(x) \sum_{i=1}^d b_i(x) \frac{\partial q(x)}{\partial x_i} \delta(q(x) - \zeta) dx \\ &+ \int_{\mathbb{R}^d} \sum_{i,j=1}^d \frac{\partial q(x)}{\partial x_i} \frac{\partial}{\partial x_j} (a_{ij}(x) \rho(x)) \delta(q(x) - \zeta) dx, \end{aligned}$$

where in the second step we used (3.6). Using the definition (3.16) for the equilibrium current  $J(x)$ , the two integrals in the last equality can be recombined into

$$\begin{aligned} \frac{dA(\zeta)}{d\zeta} &= - \int_{\mathbb{R}^d} \sum_{i=1}^d \frac{\partial q(x)}{\partial x_i} J_i(x) \delta(q(x) - \zeta) dx \\ &= - \int_{\partial S(\zeta)} \sum_{i=1}^d n_{\partial S(\zeta),i}(x) J_i(x) d\sigma_{\partial S(\zeta)}(x) = 0, \end{aligned} \tag{A.55}$$

where in the last equality we use the fact that the probability flux of the regular (by opposition to reactive) trajectories through any surface is zero at equilibrium. (A.55) implies that  $A(\zeta) = A(0) = k_{AB}$  for all  $\zeta \in [0, 1]$  as claimed. Hence,  $\int_0^1 A(\zeta) d\zeta = k_{AB}$  which gives

$$\begin{aligned} & \int_0^1 \int_{\mathbb{R}^d} \rho(x) \sum_{i,j=1}^d \frac{\partial q(x)}{\partial x_j} a_{ij}(x) \frac{\partial q(x)}{\partial x_j} \delta(q(x) - \zeta) dx d\zeta \\ &= \int_{\Omega_{AB}} \rho(x) \sum_{i,j=1}^d \frac{\partial q(x)}{\partial x_j} a_{ij}(x) \frac{\partial q(x)}{\partial x_j} dx = k_{AB}. \end{aligned}$$

This is (3.19).

## A.5. Short Account to Free Energy

An important quantity to characterize the transition behavior of a diffusion process in a (non-trivial) potential landscape is the *free energy* with respect to a reaction



coordinate. A reaction coordinate can be seen as an observable providing information on the progress of a reaction between a reactant state and a product state. Formally, a reaction coordinate is a continuous and smooth function  $\xi : \mathbb{R}^d \mapsto \mathbb{R}^n$  whose level sets  $\xi^{-1}(c) = \{x \in \mathbb{R}^d : \xi(x) = c\}$ ,  $c \in \mathbb{R}^n$  foliate the state space and comprise all states which are indistinguishable with respect to the reaction, respectively. In the traditional way, the free energy is defined by means of the marginal distribution of the equilibrated process with respect to a given reaction coordinate. Here we give only a short introduction to the free energy. For details see, e.g. [45, 46]. To formalize things, consider the Smoluchowski dynamics in a potential landscape

$$dX_t = -\nabla V(X_t)dt + \sqrt{2\beta^{-1}}dW_t,$$

where  $X_t \in \mathbb{R}^d$  and the remaining parameters are as in (2.37). The probability to find the equilibrated system in a certain region, say  $D \subset \mathbb{R}^d$ , is given in terms of the equilibrium density function  $\exp(-\beta V(x))$ , that is

$$\mathbb{P}(X_t \in D) = Z^{-1} \int_D \exp(-\beta V(x))dx,$$

where  $Z$  is the normalization factor.

In order to define the free energy, consider the marginal probability density function with respect to the reaction coordinate  $\xi$ , that is

$$Z(c) = \int_{\mathbb{R}^d} \exp(-\beta V(x))\delta(\xi(x) - c)dx,$$

where  $\delta(x)$  is the famous delta-function. The standard free energy is defined as the logarithm of the marginal probability density function  $Z(c)$ ,

$$\begin{aligned} V_{free} : \mathbb{R}^n &\rightarrow \mathbb{R} \\ V_{free}(c) &\stackrel{def}{=} -\beta^{-1} \log Z(c). \end{aligned}$$

## A.6. Definitions and Theorems

**Wiener process** The Wiener process  $W_t$  is a mathematical model of the Brownian motion of a free particle in the absence of friction.

**Definition A.6.1** (Wiener process and white noise). *The standard  $d$ -dimensional Wiener process  $W_t$  is a  $d$ -dimensional, time-homogeneous Markov process on  $\mathbb{R}^d$  with independent and stationary  $\mathcal{N}(0, (t-s)I)$ -distributed increments  $W_t - W_s$ , with initial value  $W_0 = 0$ , and with almost certainly continuous sample functions.*

*A  $d$ -dimensional stochastic process  $\eta$  is said to be a **white noise** if it is a Gaussian process with mean zero and covariance  $\langle \eta_i(t)\eta_j(s) \rangle = \delta_{ij}\delta(t-s)$ .*

### Existence and Uniqueness of Solution

**Theorem A.6.1.** ([3], page 105) *Suppose that we have a stochastic differential equation*

$$dX_t = b(t, X_t)dt + \sigma(t, X_t)dW_t, X_0 = c, \quad 0 \leq t \leq T < \infty, \quad (\text{A.56})$$

## A. Appendix

where  $W_t$  is standard  $d$ -dimensional standard Wiener process and  $c$  is a random variable independent of  $W_t - W_0$  for  $t \geq 0$ . Suppose that the  $\mathbb{R}^d$ -valued function  $b(t, x)$  and the  $(d \times d)$ -valued function  $\sigma(t, x)$  are measurable on  $[0, T] \times \mathbb{R}^d$  and have the following properties: There exists a constant  $K > 0$  such that

a) (Lipschitz condition) for all  $t \in [0, T], x, y \in \mathbb{R}^d$ ,

$$\|b(t, x) - b(t, y)\| + \|\sigma(t, x) - \sigma(t, y)\| \leq K\|x - y\|.$$

b) (Restriction of growth) For all  $t \in [0, T], x \in \mathbb{R}^d$ ,

$$\|b(t, x)\|^2 + \|\sigma(t, x)\|^2 \leq K^2 \|1 + \|x\|^2\|.$$

Then, equation (A.56) has on  $[0, T]$  a unique  $\mathbb{R}^d$ -valued solution  $\{X_t, 0 \leq t \leq T\}$ , continuous with probability 1, that satisfies the initial condition  $X_0 = c$ .

**Time reversal of diffusion** The following theorem on time reversal of a diffusion process  $\{X_t, 0 \leq t \leq T\}$ ,  $T > 0$  satisfying the stochastic differential equation

$$dX_t = b(t, X_t)dt + \sigma(t, X_t)dW_t,$$

where  $b : [0, T] \times \mathbb{R}^d \rightarrow \mathbb{R}^d, \sigma : [0, T] \times \mathbb{R}^d \rightarrow \mathbb{R}^{d \times d}$ , is found in [47] which generalizes results in [14].

Define the reversed time process by  $X_t^R \stackrel{def}{=} X_{T-t}$ , then

**Theorem A.6.2.** *If for almost all  $t > 0$ , the law of  $X_t$  has a probability density  $v(t, x)$  such that for all  $s > 0$  and any open bounded set  $C \subset \mathbb{R}^d$*

$$\int_s^T \int_C \|v(t, x)\|^2 + \sum_{i=1}^d \left\| \sum_{j=1}^d \sigma_{ij}(t, x) v(t, x)_{x_j} \right\|^2 dx dt < \infty,$$

where  $v(t, x)_{x_j}$  denotes the partial derivative of  $v(t, x)$  in the distribution sense, then the reversed time process  $X_t^R$  is a Markov diffusion process satisfying the SDE

$$dX_t^R = b^R(t, X_t^R)dt + \sigma^R(t, X_t^R)dW_t,$$

where

$$\begin{aligned} b_i^R(t, x) &= -b_i(T-t, x) + 2 \frac{\sum_{j=1}^d \frac{d}{dx_j} [a_{ij}(T-t, x) v(T-t, x)]}{v(T-t, x)}, \quad 1 \leq i \leq d, \\ \sigma_{ij}^R(x, t) &= \sigma_{ij}(x, T-t), \quad 1 \leq i, j \leq d, \\ a(x, t) &= \frac{1}{2} \sigma(x, t) \sigma^T(x, t). \end{aligned}$$

**Poincaré Lemma** The proof of the existence of a unique weak solution of the elliptic mixed-value boundary problem (A.40) bases on the general version of the Poincaré-Lemma.

**Theorem A.6.3.** ([20], page 127-130) Assume that the Lipschitz domain  $\Omega \subset \mathbb{R}^d$  is bounded, connected and open and the subset  $\Sigma \subset \partial\Omega$  is Lipschitz continuous and has a positive Hausdorff measure. Then there exists an  $C_\Omega > 0$  such that

$$\int_{\Omega} |\nabla v|^2 dx \geq C_\Omega \int_{\Omega} v^2 dx, \quad \forall v \in H_{\Sigma}^1(\Omega)$$

where the Sobolev space  $H_{\Sigma}^1(\Omega)$  is defined by

$$H_{\Sigma}^1(\Omega) = \{u \in H^1(\Omega) : \text{tr}_{\Sigma} u = 0\}.$$

### Hypoelliptic operators

**Definition A.6.2.** ([71], page 139) A linear second order operator  $G$  with infinitely often differentiable coefficients defined in a domain  $\Omega \subset \mathbb{R}^d$  is called **hypoelliptic** in  $\Omega$  if for any distribution  $u$  in  $D(\Omega)$  and any domain  $\Omega_1 \subset \Omega$  the condition that  $G u \in C^\infty$  implies that  $u$  is infinitely often differentiable in  $\Omega_1$ .

**Theorem A.6.4.** ([71], page 139) If the second order operator

$$G u = a : \nabla \nabla u + b \cdot \nabla u + c u$$

with real coefficients  $a_{ij}(x), b_i(x), c(x)$  in the class  $C^\infty(\Omega)$  is hypoelliptic in the domain  $\Omega$ , then for any point  $x \in \Omega$

$$\text{either } \sum_{i,j=1}^d a_{ij} \xi_i \xi_j \geq 0 \text{ or } \sum_{i,j=1}^d a_{ij} \xi_i \xi_j \leq 0$$

for all  $\xi \in \mathbb{R}^d$ .

**Theorem A.6.5.** ([96], page 9) If the operator  $(-\frac{d}{dt} + \mathcal{L}_{f,w})$  is hypoelliptic, then the law of  $X_t$  has a smooth density  $p(t, x)$  on  $(0, \infty) \times \mathbb{R}^d$ , i.e.,

$$\mathbb{P}(X_t \in dy) = p(t, y) dy,$$

and  $p(t, x)$  satisfies the Fokker-Planck equation

$$\frac{dp}{dt} = \mathcal{L}_{f,w} p.$$

**M-matrix** The following definitions and Lemmata are found in [44]. The elements of a matrix  $A$  are denoted by  $a_{ij}$ ,  $i, j \in I$ . Here  $A$  and the index set  $I$  assume the places of  $\bar{L}_h$  and  $\bar{\Omega}_h^S$ . The index  $i \in I$  is said to be *directly connected* with  $j \in I$  if  $a_{ij} \neq 0$ . We say that  $i \in I$  is *connected* with  $j \in I$ , denoted by  $i \rightarrow j$ , if there exists a *connection*

$$i = i_0, i_1, \dots, i_n = j \text{ with } a_{i_{k-1}i_k} \neq 0, \quad (1 \leq k \leq n).$$

## A. Appendix

**Definition A.6.3.** A matrix  $A \in \mathbb{R}^{I \times I}$  is called irreducible if every  $i \in I$  is connected to every  $j \in I$ .

**Definition A.6.4.** A matrix  $A \in \mathbb{R}^{I \times I}$  is called strictly diagonally dominant if

$$|a_{ii}| > \sum_{j \neq i} |a_{ij}|, \quad \forall i \in I, \quad (\text{A.57})$$

weakly diagonally dominant if

$$|a_{ii}| \geq \sum_{j \neq i} |a_{ij}|, \quad \forall i \in I, \quad (\text{A.58})$$

irreducible diagonally dominant if  $A$  is irreducible and weakly diagonally dominant and if, furthermore,

$$|a_{kk}| > \sum_{j \neq k} |a_{kj}| \quad \text{for at least one } k \in I \quad (\text{A.59})$$

and essentially diagonally dominant if  $A$  is weakly diagonally dominant and every  $i \in I$  is connected to a  $k \in I$  for which the inequality in (A.59) holds true.

Now we turn our attention to special subclass of positive matrices.

**Definition A.6.5.** A matrix  $A \in \mathbb{R}^{I \times I}$  is said to be an  $M$ -matrix if  $A$  satisfies

$$a_{ii} > 0, \text{ for all } i \in I, \quad (\text{A.60})$$

$$a_{ij} \leq 0, \text{ for all } i \neq j, \quad (\text{A.61})$$

$A$  is regular and  $A^{-1} \geq 0$  componentwise.

**Theorem A.6.6.** Let  $A \in \mathbb{R}^{I \times I}$  be strictly or essentially or irreducibly diagonally dominant. If the sign conditions (A.60), (A.61) are satisfied then  $A$  is an  $M$ -matrix.

The proofs for stability of the discretization schemes derived in Section A.1.2 and Section A.1.3 are based on the following theorem.

**Theorem A.6.7.** Let  $A \in \mathbb{R}^{d \times d}$  be an  $M$ -matrix. If a vector  $w \in \mathbb{R}^d$  exists with  $Aw \geq \mathbf{1}$  then

$$\|A^{-1}\|_{\infty} \leq \|w\|_{\infty},$$

where  $\|A^{-1}\|_{\infty} = \sup_{\|w\|_{\infty}=1} \|A^{-1}w\|_{\infty}$  is the matrix-norm with respect to the maximum norm  $\|\cdot\|_{\infty}$ .

**Two theorems on the existence of generators** The following Theorems are found in [53]. They give sufficient conditions for the existence of a generator of a given transition matrix.

**Theorem A.6.8.** Let  $P$  be a transition matrix and suppose that

(a)  $\det(P) \leq 0$ , or

(b)  $\det(P) > \prod_i p_{ii}$ , or

(c) there are states  $i$  and  $j$  such that  $j$  is accessible from  $i$ , but  $p_{ij} = 0$ .

Then, there is no generator  $L \in \mathfrak{G}$  such that  $P = \exp(L)$ .

**Theorem A.6.9.** *Let  $P$  be a transition matrix.*

- (a) *If  $\det(P) > \frac{1}{2}$ , then  $P$  has at most one generator.*
- (b) *If  $\det(P) > \frac{1}{2}$  and  $\|P - I\| < \frac{1}{2}$  (using any operator norm), then the only possible generator for  $P$  is the principal branch of the logarithm of  $P$ .*
- (c) *If  $P$  has distinct eigenvalues and  $\det(P) > e^{-\pi}$ , then the only possible generator for  $P$  is the principal branch of the logarithm of  $P$ .*